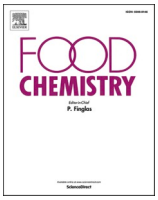
Food Chemistry 477 (2025) 143581



Contents lists available at ScienceDirect

Food Chemistry

journal homepage: www.elsevier.com/locate/foodchem





Basil chilling injury: Oxidative stress or energy depletion?

Dorthe H. Larsen [a,b,1], Ying Liu [a,*,1], Miaomiao Yao [a], Özlem Erol [d], Yongran Ji [a], Ernst J. Woltering [a,c], Leo F.M. Marcelis [a], Young Hae Choi [d]

[a] Horticulture and Product Physiology, Department of Plant Sciences, Wageningen University & Research, PO Box 16, 6700, AA, Wageningen, the Netherlands
[b] Plant and Soil Science Section, Department of Plant and Environmental Sciences, Faculty of Science, University of Copenhagen, Thorvaldsensvej 40, Frederiksberg C, DK-1871 Copenhagen, Denmark
[c] Food & Biobased Research, P.O. Box 17 6700AA, Wageningen University and Research, Wageningen, the Netherlands
[d] Natural Products Laboratory, Institute of Biology, Leiden University, 2333, BE, Leiden, the Netherlands

ARTICLE INFO

Dataset link: Data underlying the article Basil Chilling Injury: Oxidative Stress or Energy Depletion (Original data)

Keywords:
Chilling stress
Ocimum basilicum
Postharvest quality
Metabolomics
Carbohydrate metabolism
Antioxidant metabolism

ABSTRACT

Basil (*Ocimum basilicum* L.) is susceptible to chilling injury (CI), leading to significant postharvest quality loss. This research aimed to identify key metabolites involved in CI of basil during cold storage to better understand the underlying mechanisms. Metabolite profiles of basil leaves stored at 4 and 12 °C for up to 12 days were quantified by ^{1}H NMR and GC–MS. At 4 °C shelf life was reduced due to CI. At 4 °C, several osmoprotectants, including proline, gamma-aminobutyric acid, trehalose and myo-inositol increased, whereas antioxidants like ascorbic acid and rosmarinic acid decreased; the latter likely due to scavenging reactive oxygen species. During chilling stress, antioxidant defence pathways were upregulated and carbohydrate related energy pathways were downregulated. We suggest that CI in basil associates with redirection of carbohydrate flux towards antioxidant defence systems, leading to energy depletion. This energy depletion is hypothesized as a primary trigger for CI in postharvest basil.

1. Introduction

Basil (*Ocimum basilicum* L.) is an economically important herb which is widely consumed due to its distinctive flavour and appealing appearance. Originating from the tropical region, basil is inherently sensitive to chilling injury (CI) when exposed to low temperatures (< 10–12 °C) during growth and postharvest storage (Lange & Cameron, 1994; Meir et al., 1997). In contrast, many other horticultural products are not sensitive to low temperatures and consequently, to preserve quality, these products are commonly transported and stored at temperatures around 4 °C. Basil is often transported or stored together with these other products, and this may (depending on the time frame) lead to CI (Lange & Cameron, 1997). Symptoms of basil CI include leaf browning/blackening, wilting, necrosis, rot, loss of glossy appearance and a reduced abundance of total volatile emissions (Cozzolino et al., 2016). These symptoms can lead to a decrease in consumer purchase of basil and ultimately result in postharvest losses. Therefore, it is economically and scientifically important to understand the mechanism underlying CI progression for alleviating CI symptoms. Most research regarding CI has been done in fruit. In these products, the symptoms generally only appear after the fruit has been transferred from low temperature to warmer temperature (Albornoz et al., 2022). This is not the case for leaves, here the symptoms appear much quicker, within a few days in the low temperature storage (Lange & Cameron, 1994; Larsen, Li, van de Peppel, et al., 2022). In both leaves and fruit, CI intensifies with prolonged cold storage, however, the effect of storage time on CI is often not incorporated in CI studies.

At present, there are two prevailing causes for CI: one is the direct effect of low temperature on the fluidity of the cell membranes that changes from a flexible liquid phase to a solid gel phase (Liang et al., 2020), the other is the cold-induced increased oxidative stress (i.e. overaccumulation of reactive oxygen species (ROS)) (Zhang et al., 2021). The increase in ROS often includes an increase in singlet oxygen, superoxide radical, hydrogen peroxide, and hydroxyl radical (Liang et al., 2020). In addition, the activity of antioxidant enzymes may be reduced by low temperature, which impairs their ability to neutralize ROS effectively. The increase in ROS and the weakened antioxidant ability can lead to the oxidation and destruction of membrane lipids

* Corresponding author.
E-mail address: ying.liu@wur.nl (Y. Liu).
[1] These authors equally contributed to this article.

https://doi.org/10.1016/j.foodchem.2025.143581
Received 29 November 2024; Received in revised form 19 February 2025; Accepted 22 February 2025
Available online 25 February 2025
0308-8146/© 2025 The Authors. Published by Elsevier Ltd. This is an open access article under the CC BY license (http://creativecommons.org/licenses/by/4.0/).

(particularly the unsaturated fatty acids). Presumably the two determining processes (the direct effect on membrane fluidity and the increase in ROS) occur in parallel during the development of CI and the current methods to detect chilling damage (e.g. ion leakage and chlorophyll fluorescence) do not distinguish between them. Both processes lead to a loss of semi-permeability and dysfunction of cell membranes and finally cell death, as evidenced by an increase in ion leakage from the chilling injured tissue (Wright & Simon, 1973). However, the two prevailing causes alone may not fully explain the observed variations in chilling tolerance in basil. Some studies suggest that the membrane lipid composition affects the sensitivity to chilling temperatures (Cao et al., 2011; Liu et al., 2020), with some less chilling sensitive basil cultivars having higher levels of unsaturated fatty acids (Meir et al., 1995). Whereas another study found that the levels of saturated and unsaturated membrane fatty acids were similar between young and mature basil leaves, with mature leaves being less tolerant to CI (Wongsheree et al., 2009). With respect to the increased oxidative stress during cold storage, the levels of phenolic (non-enzymatic) antioxidants, such as rosmarinic acid, chicoric acid and anthocyanins, decreased in basil leaves as they were utilized for ROS scavenging (Fratianni et al., 2017; Larsen, Li, van de Peppel, et al., 2022). However, phenolic antioxidants likely play little role in improving chilling tolerance in basil, probably due to their low correlation with the overall antioxidant activity in basil leaves (Dudai et al., 2017; Larsen, Li, van de Peppel, et al., 2022; Noguchi et al., 2005). In contrast, enzymatic antioxidants such as catalase have been reported to improve chilling tolerance (Wongsheree et al., 2009).

In addition to the two prevailing causes related to cell membrane damage and oxidative stress, carbohydrates are also suggested to play a role in chilling resistance. Soluble sugars are assumed to stabilize cell membranes, regulate osmotic pressure, and remove ROS through their antioxidant properties (Sami et al., 2016). Basil leaves fed with sucrose or glucose solution were more tolerant to cold (Afrina et al., 2012). An increase in leaf carbohydrate levels due to application of additional far-red light during cultivation also improved the chilling tolerance in basil leaves (Larsen et al., 2023). In peach fruit, an increase in soluble sugar content, particularly sucrose, has been correlated with improved resistance to chilling stress (Zhao et al., 2022).

Despite the enumerated extensive research on CI, numerous long-standing challenges persist, hindering complete understanding of the precise mechanism underlying CI. Research in this area often appears fragmented, with many studies focusing on symptom alleviation through external treatments rather than deepening the understanding of the internal mechanism. Particularly the role of primary and secondary metabolites in the development of CI is unclear. We aimed at a deeper understanding of the CI progression in postharvest basil by studying the metabolites-related biochemistry. For this purpose, we analysed the changes of metabolites over time in chilled and non-chilled basil leaves using ^{1}H NMR and GC–MS metabolomics platforms.

2. Materials and methods

2.1. Plant growth

Basil plants (*Ocimum basilicum* L., cv. Dolly, Enza Zaden, the Netherlands) were cultivated twice in time in two compartments of a climate chamber, using the same chamber as described by Larsen, Li, van de Peppel, et al. (2022). In brief, seeds were sown in stone wool plugs (Grodan Rockwool B.V., Roermond, the Netherlands), one per plug, and transplanted after 15 days into 7.5 × 7.5 × 6.5 cm stone wool blocks at a density of 123 plants m^{-2}. Plants were cultivated under red-white light emitting diodes (LEDs) (GreenPower PM-DR/W-120, Philips, Eindhoven, the Netherlands) with 7 % blue (400–500 nm), 16 % green (500–600 nm), 76 % red (600–700 nm) and 1 % far-red (700–800 nm). The photosynthetic photon flux density (PPFD) was maintained at 196 ± 12 µmol m^{-2} s^{-1} at the top of the canopy and the photoperiod was 18 h. The day/night temperature was maintained at 25 °C, the relative humidity was kept at 70 %, and the CO_2 concentration was ambient. Plants were watered with an ebb and flood system using a nutrient solution (8.5 mM NO_3^-, 3.9 mM SO_4^{2-}, 1.5 mM HCO_3^-, 1.5 mM HPO_4^{2-}, 1.5 mM NH_4^+, 5.5 mM K^+, 4.0 mM Ca^{2+}, 1.5 mM Mg^{2+}, 0.2 mM Cl^-, 30 µM Fe^{3+}/Fe^{2+}, 5 µM Mn^{2+}, 5 µM Zn^{2+}, 35 µM $H_2BO_3^-$, 1 µM Cu^+/Cu^{2+}, 1 µM MoO_4^{2-}) at pH 5.7 and EC 1.7 dS m^{-1} before transplanting. After transplanting the EC was raised to 2.3 dS m^{-1} by proportionally increasing all nutrient concentrations.

2.2. Postharvest storage and sampling

A total of 144 uniform non-border plants were harvested 20 days after transplanting from two growth cycles. Detailed statistical information is provided in section 2.5. At harvest, the top two fully developed leaf pairs from each plant were harvested. Postharvest storage was performed as described by Larsen, Li, van de Peppel, et al. (2022). In brief, harvested leaves from two plants were stored in one plastic box that was equipped with wetted filter paper to maintain a high relative humidity and a lid with small holes to ensure sufficient exchange of air to avoid a built up of CO_2 and ethylene. After each growth cycle, boxes containing leaves harvested from the same growing compartment were evenly distributed without biased selection into one of the two dark cabinets at a chilling temperature of 4 °C and one of the two dark cabinets at a non-chilling temperature of 12 °C. In the boxes the temperature and relative humidity deviated within ±0.3 °C and 2 % as recorded by keytag dataloggers (KTL-508, Keytag, Leiderdrop, the Netherlands). Non-destructive measurements, namely overall visual quality (OVQ) and maximum quantum yield of PSII (Fv/Fm), and destructive sampling were conducted on day 0 (at harvest), 3, 6, 9, and 12 after harvest. After the non-destructive measurements, leaves from two boxes (four plants) were pooled as one sample, quickly frozen in liquid nitrogen and stored at −80 °C, resulting in a total of 36 samples. The samples were ground under liquid nitrogen and freeze-dried before further metabolomic analysis.

2.3. Non-destructive measurements

2.3.1. Overall visual quality (OVQ)

The assessment of OVQ employed a scoring system that relied on visual symptoms associated with CI, as well as senescence symptoms observed at non-chilling temperatures. The OVQ score ranges from 8 (high quality, no defects) to 1 (fully decayed leaves, wilted, black) where 5 (clear brown or black coloration, or first signs of senescence) was designated as the customer acceptance limit, representing the end of shelf life. The evaluation principle was as described by Larsen, Li, van de Peppel, et al. (2022) (Supplementary Table S1).

2.3.2. Maximum PSII efficiency (Fv/Fm)

Chlorophyll fluorescence parameter Fv/Fm ratio defines the maximum quantum yield of Photosystem II (PSII) performed on dark-adapted leaves. This ratio is employed as a sensitive indicator of plant photosynthetic performance, particularly with lower values indicating stresses. Fv/Fm is used in this study to quantify CI (Meir et al., 1997). The leaves were dark-adapted for 20 min at room temperature after which the Fv/Fm of all leaves per box was measured using chlorophyll fluorescence imaging (Fluorcam 800-C, PSI, Drásov, Czech Republic) as described by Larsen, Li, van de Peppel, et al. (2022).

2.4. Metabolic analysis

The metabolomics investigation encompassed two phases: an initial comprehensive metabolic profiling utilizing ^{1}H NMR spectroscopy, coupled with microscopic analysis of primary, secondary and volatile metabolites via GC–MS. This methodology enabled the characterization of both the broader metabolic landscape and the intricate details within

basil leaves. Note that biological (not technical) replicates were used in the following metabolic analyses.

2.4.1. NMR analysis

For NMR analysis, basil samples were extracted by two kinds of solvents: CH_3OH-d_4, and the mixture of CH_3OH-KH_2PO_4 buffer in D_2O (1:1, *v*/v). The aqueous extracts covered more polar metabolites such as carbohydrates, amino acids, organic acids, and some polar phenolics; the methanolic extract was for lipids and terpenoids. Thirty mg of freeze-dried basil samples were vortexed for five seconds either with 1 mL of CH_3OH-d_4 containing 0.418 mM of hexamethyldisiloxane (HMDSO) as an internal standard, or 1 mL of CH_2OH-d_4 – KH_2PO_4 buffer in D_2O (90 mM, pH 6.0, 1:1, v/v) containing 0.29 mL of trimethysilylpropionic acid sodium salt (TMSP) as an internal standard, and then ultrasonicated for 20 min. The resulting extracts were centrifuged at 17,000 × *g* for 20 min and 300 μL aliquots of the supernatants were transferred to 3 mm NMR tubes for ^{1}H NMR analysis. The ^{1}H NMR analysis was carried out with an AV-600 MHz NMR spectrometer (Bruker, Karlsruhe, Germany), operating at a proton NMR frequency of 600.13 MHz. For internal locking, CH_3OH-d_4 was used. All ^{1}H NMR measurements consisted of 64 scans requiring 10 min and 26 s as acquisition time using the parameters of 0.16 Hz/point, pulse width (PW) = 30° (11.3 μs), and relaxation time of 1.5 s. A pre-saturation sequence was used to suppress the residual water signal using low power selective irradiation at H_2O frequency during recycle delay. The free induction decays (FIDs) were Fourier transformed with exponential line broadening of 0.3 Hz. The resulting spectra were manually phased, and baseline corrected and calibrated to HMDSO at 0.06 ppm using TOPSPIN V. 3.0 (Bruker).

2.4.2. GC–MS analysis

Basil samples were analysed for aqueous methanolic extracts and volatiles by using a 7890A gas chromatograph equipped with a 7693 automatic sampler and a 5975C single quadrupole detector (Agilent, Folsom, CA, USA).

For the analysis of aqueous methanolic extracts, 30 mg of freeze-dried basil samples were extracted with 1 mL of the solution of MeOH-H_2O (1:1, *v*/v) with 10 s vortex and 20 min ultrasonication at 25 °C. The extracts were centrifuged for 10 min at 17,000 × *g*. Three hundred μL of supernatant was transferred into a 1.5 mL glass vial and dried in a speed vac (Labonco, Kansas City, MO, USA). The dried extracts were redissolved in 100 μL of methoxyamine hydrochloride solution in pyridine (20 mg/mL) and reacted at 40 °C for 2 h. The reactants were further TMS-derivatized by the addition of 140 μL of *N*-Methyl-*N*-(trimethylsilyl)trifluoroacetamide (MSTFA) at 40 °C for 2 h. The samples were analysed by the GC–MS with a DB-5 GC column (30 m × 0.25 mm, 0.25 μm film, J&W Science, Folsom, CA, USA) and eluted with helium (99.9 % purity) as a carrier gas at a flow rate of 1.5 mL/min. The oven temperature was programmed: after an initial hold at 60 °C for 1 min, increased at 7 °C/min to 290 °C, and held for 5 min; then increased to 310 °C at 5 °C/min and held for 3 min. The injector was set at 280 °C and 1 μL of the sample was injected in splitless mode. The interface temperature was set at 280 °C, and the ion source and quadrupole temperature were 230 °C and 150 °C, respectively. The ionization energy in EI mode was 70 eV.

The same set of basil leaves were analysed by headspace GC–MS for their volatiles. Seventy mg of dried samples were placed into a 20 mL headspace vial with 5 μL of tridecane (1 mg/mL) as an internal standard followed by incubating at 150 °C for 30 min at 650 g, and 500 μL of the headspace were injected to the GC–MS system (Agilent) with a 20:1 split ratio and 8 mL/min. Samples were separated on a DB-5 GC column (30 m × 0.25 mm, 0.25 μm film, J&W Science) and eluted with helium (99.9 % purity) as a carrier gas at a flow rate of 3.0 mL/min. The oven temperature was programmed to start at 60 °C for 1 min, increased at 7 °C/min to 200 °C and held for 2 min, then increased to 210 °C at 5 °C/min with 1 min holding. The injector, interface, and ion source temperatures were set at 280, 230, and 150 °C, respectively. The ionization energy in EI mode was 70 eV.

2.5. Data processing and statistical analysis

The experiment was analysed as a completely randomized block design. The complete experiment was carried out as two independent experiments, each using one climate chamber with two growing compartments, and two storage cabinets per temperature for the postharvest treatments. Harvested basil leaves from one growing compartment were evenly stored in one cabinet at 4 °C and one cabinet at 12 °C, resulting in one block. In total, there were four blocks as a source of variation for statistical analysis ($N = 4$). For each temperature and sampling day combination in each block, there were four plants. The OVQ and Fv/Fm data were analysed as three blocks ($N = 3$) as by accident only the average value of block one and two were noted. Linear regression was fitted for OVQ and Fv/Fm data, respectively, over time for samples stored at 4 °C and 12 °C. Differences in regression parameters were tested at the level of *P-value* < 0.05 to determine whether fitted lines differed between two temperature treatments. Shelf life was estimated using the fitted regression equations for OVQ at 4 °C and 12 °C, setting y = 5 (the threshold for acceptable quality) and solving for x (days of storage, namely shelf life). Normality and homogeneity of residuals of the variables were tested and confirmed by the Shapiro-Wilk test and the Bartlett's test, respectively. The eugenol level of the samples was analysed with two-way ANOVA with storage temperature (4 and 12 °C) and time (3, 6, 9, and 12 day) as two factors. Due to dissatisfaction on the assumption of homogeneity, data transformation of $\log_{10}$ (eugenol+1) was applied. Fisher's protected LSD was used as post-hoc test to determine significant differences between the mean values at the level of *P-value* < 0.05. Regression analysis, ANOVA and post-hoc analysis were conducted with Genstat (22nd Edition, VSN International Ltd., Hemel Hempstead, UK).

The ^{1}H NMR spectra were bucketed using AMIX 3.9.12 (Bruker BioSpin GmbH, Rheinstetten, Germany). Bucketed data were obtained by spectral integration at 0.04 ppm intervals. Peak intensity of individual peaks was scaled to total intensity and recorded from δ 0.20 to 10.02. Residual signals of D_2O and CH_3OH-d_4, in the δ 4.75 – δ 4.9 and δ 3.28 – δ 3.34 regions were excluded from the analysis, respectively.

The raw GC–MS data files of TMS-derivatized samples were converted using MSconvert (Proteowizard) to mzML format (Chambers et al., 2012). The converted files were processed using MSHub on the Global Natural Product Social Molecular Networking (GNPS) Platform and the detected peaks were identified by molecular networking (Aksenov et al., 2021; Wang et al., 2016). GC–MS data was filtered by removing all MS/MS fragment ions within ±17 Da of the precursor *m/z*. Additionally, MS/MS spectra were window-filtered by choosing only the top six fragment ions within a ±50 Da window across the spectrum. The precursor ion mass tolerance was set to 20,000 Da and the MS/MS fragment ion tolerance was set to 0.5 Da. Library spectra were filtered in the same manner as the input data. Only matches between network spectra and library spectra with a score above 0.5 and at least six matched peaks were retained for further analysis. For compound identification, nominal mass and fragmentation patterns were used, as the system was equipped with a single quadrupole mass detector. Molecular networking was applied as a visualization approach in untargeted mass spectrometry (MS), where the outcomes manifest as networks of interconnected MS/MS spectra. The mass value, retention time and cosine score of each compound are provided in Supplementary Table S4. For Headspace GC–MS data acquisition, all the total ion chromatograms were automatically integrated and peaks were identified using Mass Hunter (B.07, Agilent). All of the identified signal intensities were normalized to that of the internal standard (tridecan). Compounds were identified using NIST MS library (version 2008). Missing values in the datasets were handled by a zero-filling approach, following standard metabolomics practices.

This study did not include specific quality control samples. Instead,

two alternative quality control measures were implemented to ensure data reliability: (1) instrument performance checks, including routine calibration, tuning, and blank runs, were conducted before and during the runs to monitor and maintain instrument stability; (2) retention time locking was performed using an internal standard (methyl palmitate) or consistent retention time windows to track chromatographic shifts and ensure data consistency.

Multivariate data analysis was performed using SIMCA P (v.16.0, Umeå, Sweden). The aqueous spectra and methanolic spectra of ^{1}H NMR were combined to a single matrix for each sample to cover a broad range of metabolites. Principal component analysis (PCA) and orthogonal partial least square (OPLS) analysis were conducted for ^{1}H NMR and GC–MS data. In each dataset, two OPLS models were constructed using y variables of temperature and time, respectively. For PCA and OPLS analyses, the data was scaled using the Pareto scaling method. The validity of OPLS models was confirmed through permutation tests with 100 number of permutations and assessment of Q2 values as well as *P-value* of CV-ANOVA tests, surpassing the higher than 0.5 for Q2 values and less than 0.01 for *P-value* of CV-ANOVA. The Variable Importance in Projection (VIP) score represents the overall contribution of a variable to the OPLS model. It is calculated as a weighted sum of the squares of the Partial Least Squares (PLS) loadings, reflecting the variable's ability to explain both the response (class distinction) and the variance in the GC–MS data. A high VIP score means that the metabolite has a strong influence on the classification performance of the model. VIPs with a score > 1 were selected. Two-way ANOVA and KEGG pathway enrichment analyses for GC–MS detected compounds were performed by using MetaboAnalyst (Pang et al., 2024). Data were normalized by median, log transformed by base 10 and scaled using Pareto method. Significantly differentially expressed metabolites (DEMs) were selected based on two-way ANOVA, including compounds that showed significant differences (false discovery rate (FDR)-adjusted *P-value* < 0.05) for either the individual effects of temperature and/or time, or their interactions. The KEGG pathway enrichment analyses were conducted using the quantitative enrichment analysis option (FDR-adjusted *P-value* < 0.05), based on the temperature factor while excluding the time factor to avoid limited sample size and inaccurate results. Heatmaps were generated using WeiShengXin (Tang et al., 2023) with hierarchical clustering, employing complete linkage and the maximum distance methods.

3. Results

3.1. Shelf life and chilling injury

Leaf OVQ values decreased linear with time of storage at both temperatures, with a more rapid decline observed at 4 °C than at 12 °C (Fig. 1A). At 4 °C the Fv/Fm of leaves reduced during storage similarly as the OVQ, whereas Fv/Fm hardly changed with storage time at 12 °C (Fig. 1B). At 12 °C, the quality loss was reflected as wilting and water loss, whereas at 4 °C clear symptoms of CI such as dark spots on the leaf surface occurred within three days (Supplementary Fig. S1). The OVQ value of basil leaves at 4 °C fell below the consumer acceptance limit (score = 5) after 7 days (Fig. 1A & Supplementary Table S2) indicating the end of shelf life. The OVQ values at 12 °C stayed above the acceptance limit throughout the 12 days of storage, with an estimated shelf life of 16 days (Supplementary Table S2). The major difference in shelf life at 4 and 12 °C was caused by CI. Volatile organic compounds (VOC) are important for the aroma of basil. The major basil VOC, eugenol (56 % of total VOCs at harvest), decreased faster when leaves were stored at 4 °C compared to 12 °C (Fig. 1C).

3.2. Initial overall metabolic profiling by ^{1}H NMR

All basil samples in this study underwent an initial scan using ^{1}H NMR spectroscopy to discern the metabolic distinctions linked to postharvest temperature variations (4 and 12 °C) over different time intervals (0, 3, 6, 9, and 12 days). The metabolite profile of basil leaves could roughly be distinguished by temperature, but clear differentiation among samples collected at various time points during storage did not emerge from the PCA analysis (Supplementary Fig. S2). To further capture inherent data variations through dimensionality reduction, a supervised multivariate data analysis technique, OPLS modelling, was employed, using the same ^{1}H NMR dataset but incorporating y-variables by temperature and time, respectively (Fig. 2). These analyses demonstrated that both temperature and time distinctly impacted the metabolite profile of basil leaves. This clear effect highlighted the need for additional analysis to delve deeper into identifying individual metabolites, as the ^{1}H NMR spectroscopy is more adept at detecting different metabolite groups. The ^{1}H NMR signals indicated that most carbohydrates and amino acids exhibited susceptibility to the combined effects of temperature and time, whereas lipids, fatty acids, and flavonoids, exhibited minimal susceptibility to chilling storage (data now shown).

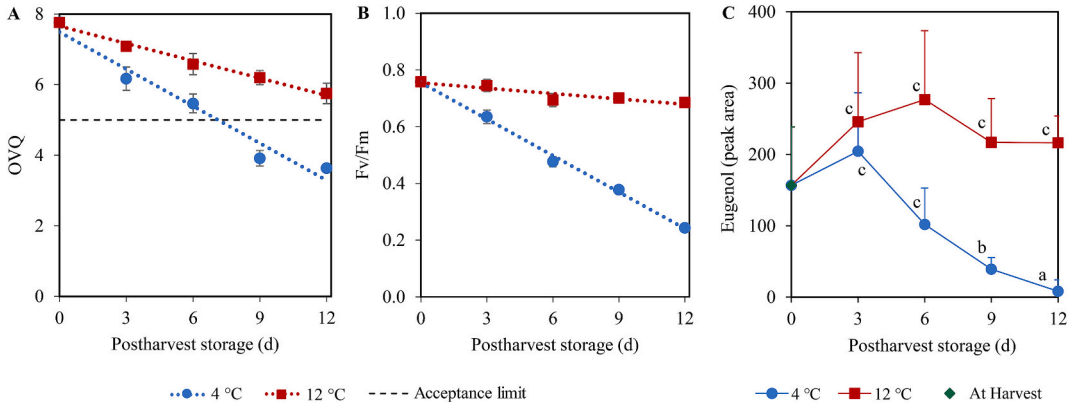


Fig. 1. Changes in quality attributes of basil. Leaves were stored at 4 °C (blue, dots) or 12 °C (red, squares) for 0 (at harvest), 3, 6, 9, 12 days in darkness. **(A)** Changes in overall visual quality (OVQ). When the OVQ values fall below the consumer acceptance limit (black dash line, OVQ = 5) it indicates the end of shelf life. **(B)** Changes in maximum quantum yield of PSII of dark-adapted leaves (Fv/Fm). The low Fv/Fm value is an indication of chilling injury (CI). **(C)** Changes in eugenol content. Data are means of blocks ($N_{OVQ} = 3$, $N_{Fv/Fm} = 3$, $N_{eugenol} = 4$). Error bars represent the standard error of the mean, visible when larger than symbol. The dotted lines in (A) and (B) are fitted linear regressions for each temperature. (C) is made based on GC–MS peak area (untransformed data), but significant differences as indicated by letters are obtained from two-way ANOVA using $\log_{10}$ (eugenol+1) transformed data (*P*-value < 0.05). (For interpretation of the references to colour in this figure legend, the reader is referred to the web version of this article.)

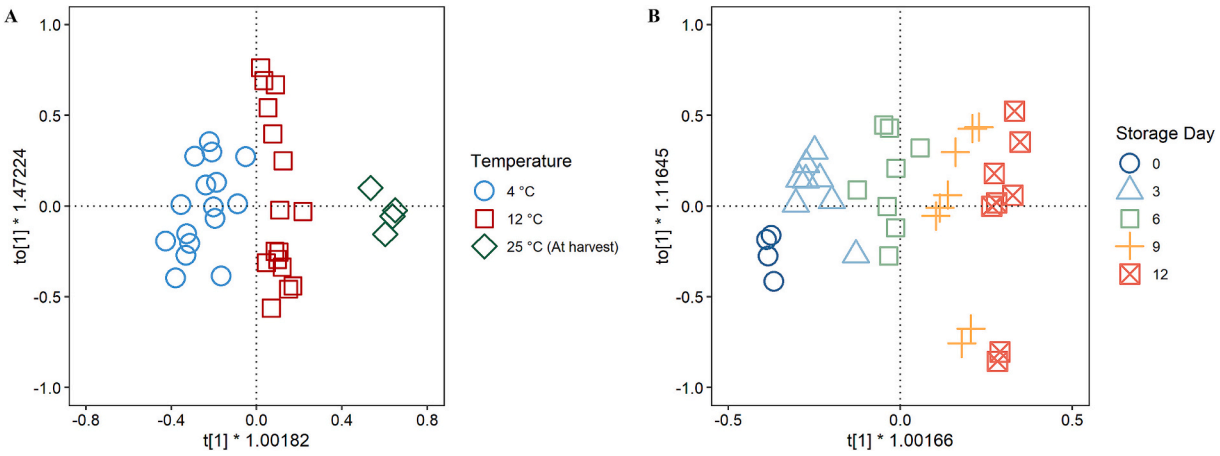


Fig. 2. Score plot of OPLS modelling based on ^{1}H NMR spectra showing the separation of basil samples. (**A**) Separation by temperature (4, 12, and 25 °C) as y-variable. (**B**) Separation by storage time (0, 3, 6, 9, and 12 day) as y-variable. The at-harvest samples (day 0) were cultivated at 25 °C, they were the initial point of the postharvest storage. The x-axis (t[1] * scaling factor) represents the scaled first predictive component related to temperature (A) or time (B), and the y-axis (to[1] * scaling factor) represents the scaled first orthogonal component, capturing variance unrelated to temperature or time effect. The scaling factors are applied for better visualization. Two distinct OPLS models were validated through Q2 values ($Q2_{temperature} = 0.79$, $Q2_{time} = 0.92$), permutation tests, and *P-value* of CV-ANOVA ($P\text{-}value_{temperature} = 3.42 \times 10^{-6}$, $P\text{-}value_{time} = 1.67 \times 10^{-12}$).

3.3. Detailed metabolic analysis using GC–MS: Highlighting changes in energy metabolism in response to chilling temperature

An in-depth exploration of metabolites was conducted via GC–MS analysis, as GC–MS provides more precise identification of individual metabolites. Four significantly different classes of metabolites were identified—carbohydrates, amino acids, organic acids, and phenolics—totalling 76 metabolites (Supplementary Table S3). The level of identification of the 76 metabolites were level two or three as described by Sumner et al. (2007) (Supplementary Table S4). Similar to the analysis approach used for ^{1}H NMR, the GC–MS dataset also underwent OPLS modelling. Herein, the storage temperature and time served as the respective y-variables (Fig. 3A,B). The sample separation either by temperature or time was validated, although the separation pattern was not as clear as the ^{1}H NMR-based OPLS modelling (Fig. 2), possibly due to the larger quantity of metabolites detected by ^{1}H NMR.

In addition to the established individual influence of temperature and time on the metabolic changes in basil leaves by both ^{1}H NMR and GC–MS techniques, the temperature and time effects appeared interactive. The deciphering of specific metabolites distinguishing samples across storage temperature and time was achieved through a shared and unique structures (SUS)-plot that obtained from the two combined OPLS models in Fig. 3A,B, revealing intricate relationships (Fig. 3C). Metabolites situated along the temperature axis (x-axis) or time axis (y-axis), ranging from negative to positive values, showed an increase in the content in response to rising temperature or time, respectively. Notably, in the SUS-plot, the major types of carbohydrates and amino acids located in the negative region of x-axis exhibited accumulations associated with chilling temperatures. For example, most of the soluble sugars and the cold-protective compounds, such as alanine and proline, accumulated at chilling temperatures, whereas glucose and ascorbic acid showed relative high abundance at non-chilling temperatures.

Among all the identified metabolites, the VIP compounds and significant DEMs affected by storage temperature and/or time were selected and visualized using a heatmap to contrast metabolite profile between chilling and non-chilling temperatures during storage (Fig. 4). The relative levels of metabolites displayed in the heatmap approximately matched their distribution shown in Fig. 3C. Of particular interest, at 4 °C, the levels of glucose 6-phosphate, ribose 5-phosphate and proline elevated from day 3, and the levels of melibiose, trehalose, gamma-aminobutyric acid (GABA), alanine, and cellobiose, increased from day 6, at the time the chilling damage was already quite severe (approximately at the end of shelf life). Conversely, the accumulations of ascorbic acid, glucose, fructose 6-phosphate, rosmarinic acid, caffeic acid and many organic acids were inhibited at 4 °C.

To comprehensively understand the regulation of metabolic pathways in response to chilling temperature, KEGG pathway enrichment analyses were first conducted for upregulated and downregulated metabolites in 4 °C compared to 12 °C, respectively, using identified VIP compounds and DEMs (Fig. 5). These analyses revealed chilling-induced enrichment in several pathways related to carbohydrate metabolism, energy utilization, cellular redox balance, amino acid metabolism, and cell membrane and cell wall metabolism. All the pathways displayed in Fig. 5 were significantly up- or downregulated (FDR < 0.05). The top three upregulated pathways are propanoate metabolism, citrate cycle (TCA cycle), and starch and sucrose metabolism (Fig. 5A), and the top three downregulated pathways are glycolysis/gluconeogenesis, tyrosine metabolism, and sphingolipid metabolism (Fig. 5B). Among all enriched pathways, the starch and sucrose metabolism, pentose phosphate pathway, glyoxylate and dicarboxylate metabolism, and glycine, serine and threonine metabolism were enriched in both upregulated and downregulated mode. Thus, a more focused second round of KEGG pathway enrichment analyses was conducted using the overlapping metabolites of VIP compounds and DEMs to determine their predominant regulatory direction. Pathways enriched in the second round were marked with yellow triangles in Fig. 5, and they were unique to either the upregulated or downregulated categories. In addition, the upregulated enrichment ratios of the starch and sucrose metabolism ($ratio_{up} = 9.45 > ratio_{down} = 3.95$) and the pentose phosphate pathway ($ratio_{up} = 9.34 > ratio_{down} = 5.60$) were higher than their downregulated enrichment ratios, while the opposite was true for the glyoxylate and dicarboxylate metabolism ($ratio_{up} = 5.26 < ratio_{down} = 7.85$) and the glycine, serine, and threonine metabolism ($ratio_{up} = 5.26 < ratio_{down} = 9.30$). Therefore, the starch and sucrose metabolism and the pentose phosphate pathway were considered more upregulated, while the glyoxylate and dicarboxylate metabolism and the glycine, serine, and threonine metabolism were considered more downregulated in response to chilling temperatures.

4. Discussion

The primary postharvest quality loss in basil is due to chilling temperatures (Brindisi & Simon, 2023), which often occurs within a few days of storage at temperatures below 10–12 °C. Basil leaves stored at

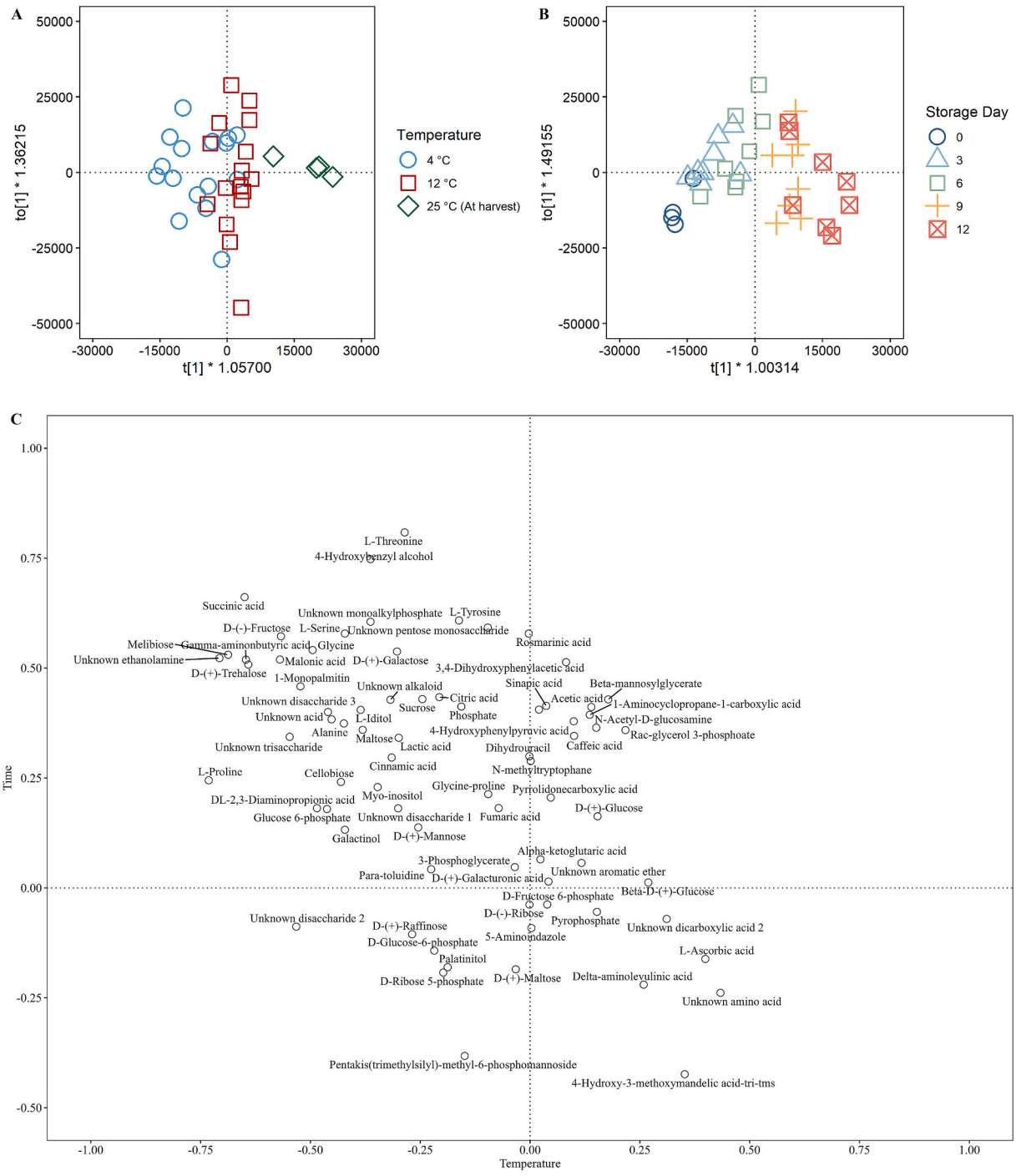


Fig. 3. Score of OPLS modelling based on GC–MS spectra showing the separation of basil samples. (**A**) separation by temperature (4, 12, and 25 °C) as y-variable; (**B**) separation by time (0, 3, 6, 9, and 12 day) as y-variable. The at-harvest samples (day 0) were cultivated at 25 °C, they were the initial point of the postharvest storage. The x-axis (t[1] * scaling factor) represents the scaled first predictive component related to temperature (A) or time (B), and the y-axis (to[1] * scaling factor) represents the scaled first orthogonal component, capturing variance unrelated to temperature or time effect. The scaling factors are applied for better visualization. Two distinct OPLS models were validated through Q2 values ($Q2_{temperature} = 0.52$, $Q2_{time} = 0.77$), permutation tests, and *P-value* of CV-ANOVA ($P\text{-}value_{temperature} = 4.74 \times 10^{-3}$, $P\text{-}value_{time} = 3.45 \times 10^{-8}$). (**C**) The shared and unique structures (SUS) plot comparing two OPLS models based on GC–MS detected metabolites. The values from negative to positive along x-axis indicates the increase in temperature and along y-axis indicates the increase in time.

chilling temperature exhibited a faster OVQ loss and shorter shelf life (Fig. 1A & Supplementary Table S2) associated with a greater decrease in Fv/Fm (Fig. 1B), compared to basil leaves stored at non-chilling temperature. This is consistent with our previous findings (Larsen, Li, Shrestha, et al., 2022; Larsen, Li, van de Peppel, et al., 2022). In addition, the level of the most abundant VOC in cv. Dolly basil samples, eugenol, showed a marked decrease during chilled storage whereas the level remained constant during storage at non-chilling temperature (Fig. 1C), leading to a pronounced decline in organoleptic quality. This VOC reduction in the cold is in line with previous studies (Cozzolino et al., 2016; Rodeo & Mitcham, 2023). Considering these findings, the detrimental impact of CI on the commercial value of basil underlines the necessity of our research in advancing the understanding of the CI mechanism. While previous studies identified general contributors to CI,

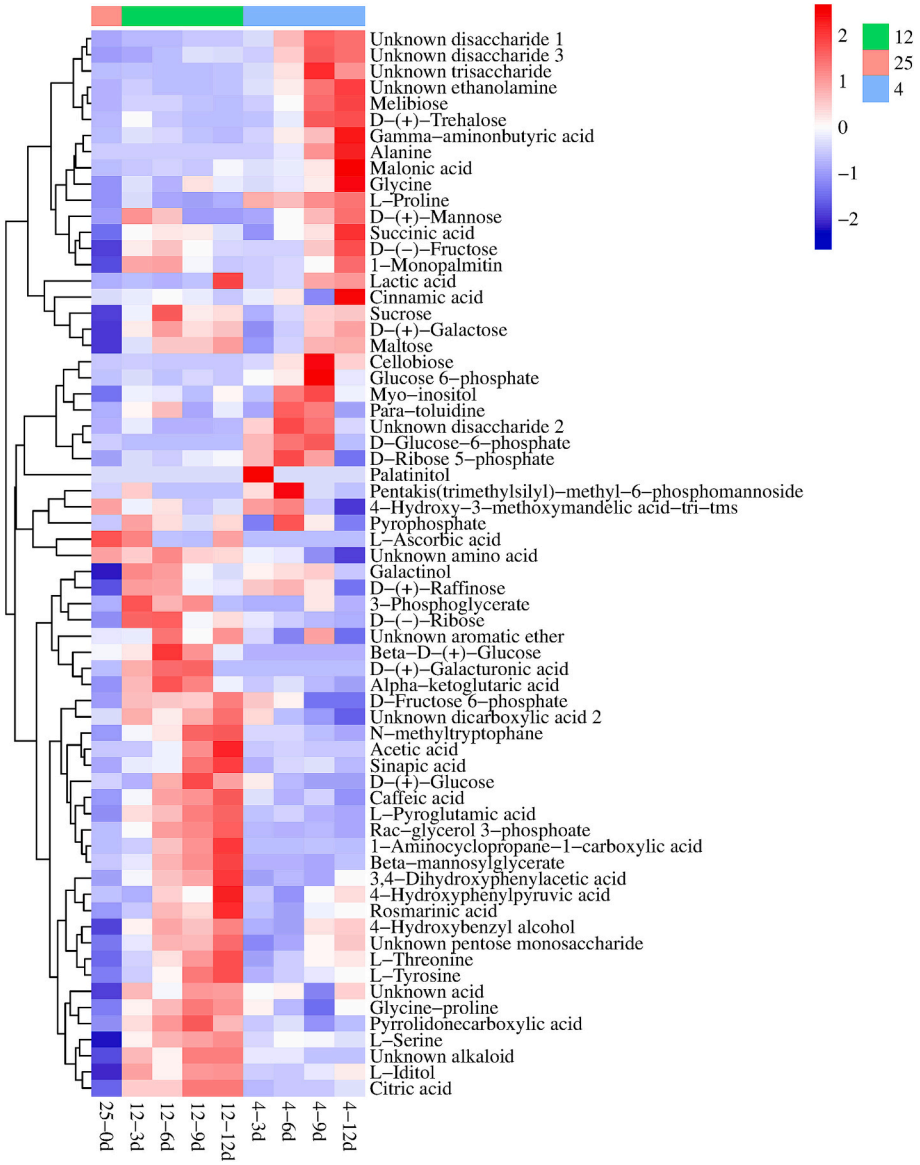
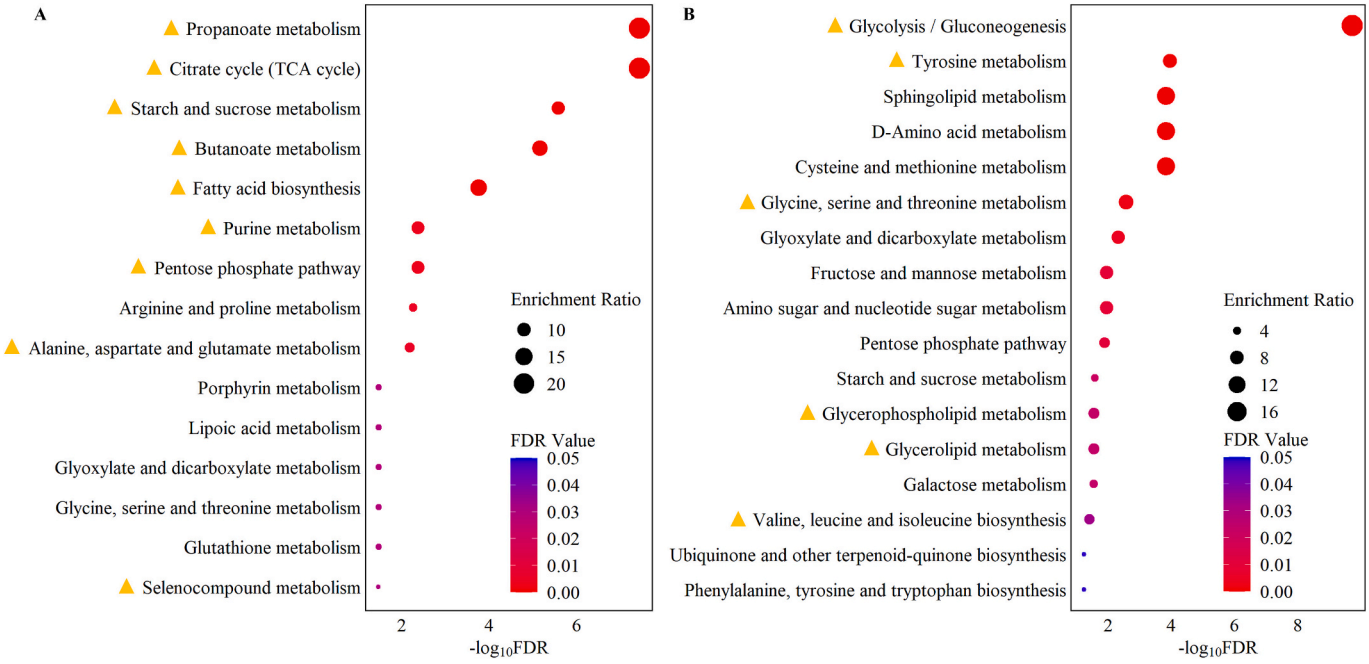


Fig. 4. Key metabolites including the variable importance of projection (VIP) compounds and significantly differentially expressed metabolites (DEMs) in basil leaves detected by GC–MS varied in different temperature and time based on VIP score > 1 and two-way ANOVA (FDR < 0.05). The values in the heatmap are standardized using z-scores, which standardize the data by subtracting the mean and dividing by the standard deviation for each row. This transformation centres the data around zero, with values representing the number of standard deviations away from the mean. Positive z-scores indicate values above the mean, while negative z-scores represent values below the mean.

the specific metabolic pathways involved remain poorly understood. In this study, we provide novel insights by linking CI in basil with a redirection of carbohydrate flux towards the antioxidant defence system, leading to energy depletion. In light of our insights into metabolic disruptions, we propose a hypothesis that energy depletion serves as a primary trigger for CI in postharvest basil leaves. Noteworthy, many of the inferences made in this study rely on enriched metabolic pathways, but we lack comprehensive measurements of all compounds within these pathways in basil, and therefore several discussions presented here remain conceptual.

4.1. *Adaptive osmoprotection and antioxidant defence*

Acknowledging that prolonged cold storage worsens the CI symptoms and that senescence and decay continue with storage time even at optimal temperatures (Albornoz et al., 2022), we not only confirmed the individual effects of chilling temperature and storage time on the metabolite profile of basil leaves (Fig. 2 & Fig. 3), but also disentangled their combined effects (Fig. 3C & Fig. 4). Essential amino acid osmoprotectants, such as proline and GABA (Zhang et al., 2021), which play roles in osmotic adjustment and structural protection, increased over time in basil leaves subjected to chilling stress (Fig. 3C & Fig. 4). Moreover, most soluble sugars (except glucose) and sugar alcohols accumulated under chilling temperature, especially those recognized as osmoprotectants, such as trehalose, mannose and myo-inositol (Li, Yong, et al., 2019; Majumder et al., 2010). The sugar-related osmoprotectants were particularly detected at the later phase of storage when the CI was more intense (Fig. 1 & Fig. 3C). The upregulation of these compounds has also been reported in peach fruits with enhanced postharvest chilling tolerance following exogenous applications of brassinosteroids or glycine betaine (Lurie, 2022). Furthermore, low levels of glucose (0.1–0.5 mM) have been reported to act as signalling molecule and effectively inducing proline accumulation (Hu et al., 2012). This report matched our depleted glucose concentration and increased



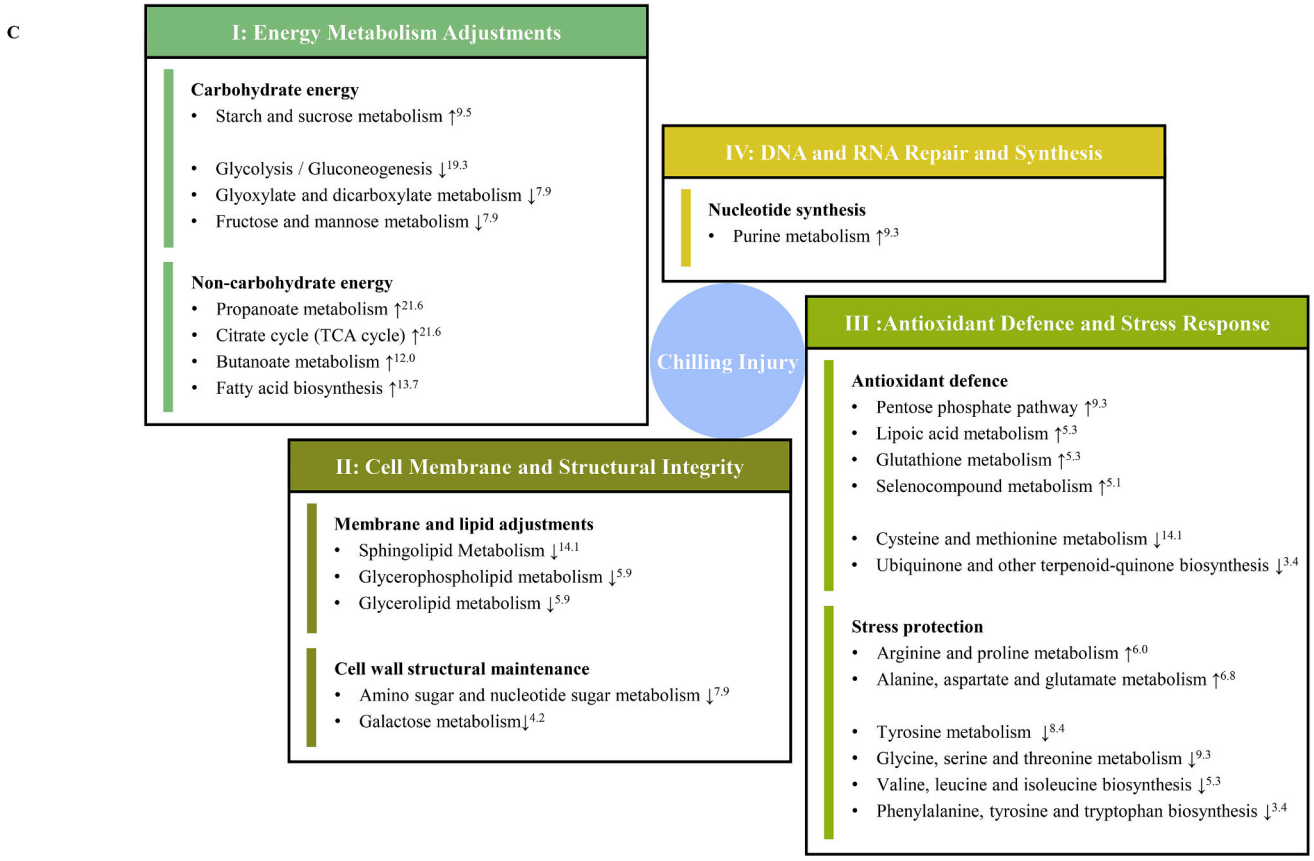


Fig. 5. KEGG pathway enrichment analysis of basil leaves stored at 4 °C compared to 12 °C using identified VIP compounds and DEMs. **(A)** upregulated pathways; **(B)** downregulated pathways. The y-axis represents enriched KEGG pathways (FDR < 0.05), the x-axis represents the -$\log_{10}$ FDR, the colour of dots indicates the FDR values, and the size of the dots represents the enrichment ratio. The enrichment ratio represents the degree of pathway enrichment compared to the background reference, with values greater than 1 signifying higher enrichment. **(C)** Summary of enriched KEGG pathway based on their functions. The pathways in each subgroup (marked by a coloured bar) are ordered by significance level from high to low. Upregulations are indicated by upwards arrows (↑) and the downregulations by downwards arrows (↓). The enrichment ratio of each pathway is labelled as a superscript after the arrows.

proline accumulation; for example, an 87 % reduction in glucose and a 468 % increase in proline were observed at 4 °C compared to 12 °C by day 6 of the shelf life (Fig. 4). Given the importance of osmoregulation in maintaining cellular homeostasis and membrane integrity, the increase in osmoprotectants suggests an active modulation of osmotic pressure in postharvest basil leaves to cope with chilling stress, especially after the first few days of cold storage. This also implies a stronger level of stress on the cell membrane with continued cold storage after basil's shelf life.

The general consensus is that CI is accompanied by excess generation of ROS. Therefore, antioxidants may improve chilling tolerance due to their ability to scavenge ROS (Blokhina et al., 2003). We observed a steep decrease in the levels of ascorbic acid, rosmarinic acid and caffeic acid in basil leaves during storage at 4 °C compared to 12 °C (Fig. 4). This reduction is likely due to their role in scavenging ROS, and this aligns with the trend of a continuous decrease in antioxidants noted in our previous studies (Larsen, Li, Shrestha, et al., 2022; Larsen, Li, van de Peppel, et al., 2022). It suggests that cellular oxidative stress is intensified by chilling. However, we do not consider the low antioxidant level to be the primary trigger of CI. This is because we also previously observed that the antioxidant concentrations (rosmarinic, chicoric and ascorbic acids) appeared unrelated to chilling tolerance in basil plants treated with additional far-red or high light intensity (Larsen et al., 2023; Larsen, Li, van de Peppel, et al., 2022). Unexpectedly, in Larsen, Li, Shrestha, et al., 2022; Larsen, Li, van de Peppel, et al., 2022), we also demonstrated a marked reduction in the level of H_2O_2 at 4 °C compared to 12 °C in the same basil cultivar as employed in this study (cv. Dolly), although this seems counterintuitive given that the accumulation of H_2O_2 during chilling stress reported in other crops (Hou et al., 2021; Li, Fan, et al., 2019; Liang et al., 2020).

We inferred that H_2O_2 level would similarly decrease in this study and seek to address a potential explanation. Hypothetically, H_2O_2 may be reduced to water by peroxidases that utilize phenolics as primary electron donors ($polyphenol + H_2O_2 \rightarrow^{peroxidase} quinone + 2H_2O$) (Albornoz et al., 2022). The polyphenols are oxidized into quinones, which then polymerize to produce brown pigments. Since H_2O_2 is the only ROS capable of crossing membranes and moving among the cytosol, vacuole, and other compartments (Blokhina et al., 2003), the generation of brown pigments may occur regardless of membrane integrity, potentially in both the early and later phases of chilling storage. Because basil is rich in phenolic compounds, we hypothesize that CI symptoms of tissue browning or blackening are due to this antioxidant defence process of reducing H_2O_2. Sugars and sugar-like metabolites have been suggested to cooperate synergistically with phenolic compounds to scavenge excess H_2O_2 (Bolouri-Moghaddam et al., 2010). The low level of a large proportion of soluble sugars and sugar-alcohols in chilled basil leaves during the early phases of shelf life (Fig. 3C & Fig. 4) may be attributed to their active participation in the antioxidant defence mechanism.

4.2. Adjustment in energy metabolism pathways

The significantly up- or downregulated KEGG metabolic pathways in chilled basil leaves were classified into four groups by their functions (Fig. 5) (Kanehisa & Goto, 2000; Pang et al., 2024). Among them, group I included energy metabolism related pathways, which generally showed higher enrichment ratios. This suggests a significant adjustment occurred in energy metabolism pathways during the development of CI in basil leaves. It is well established that glucose is the prime carbohydrate energy source in eukaryotic cellular metabolism (Bolouri-Moghaddam et al., 2010). Our measurements showed a decrease in glucose levels during storage at 4 °C and an increase at 12 °C (Fig. 4), indicating that glucose got depleted in basil leaves due to chilled storage. Glycolysis is a metabolic pathway that breaks down glucose for energy production, and its first step is sensitive to inhibition under chilling temperatures (Vichaiya et al., 2022). Fructose and mannose can also enter glycolysis after being converted to intermediates in the pathway (De Rocchis et al., 2022; Stein & Granot, 2018). The downregulation of the glycolysis pathway and the fructose and mannose metabolism pathways along with the upregulation of the starch and sucrose metabolism pathways (Fig. 5) indicate a mobilization of stored carbohydrates under chilling temperature to provide glucose to compensate for the reduced glycolysis. Namely, this upregulated starch and sucrose metabolism likely involves more starch and sucrose degradation rather than synthesis, as we previously observed a continuous reduction in starch levels in basil under chilled storage (Larsen, Li, Shrestha, et al., 2022; Larsen, Li, van de Peppel, et al., 2022). Wang et al. (2013) found that peaches stored at 5 °C had more severe CI compared to those stored at 0 °C; and Yu et al. (2015) reported that peaches at 5 °C developed CI symptoms, whereas those at 10 °C did not. In both studies, the more severe CI at 5 °C was accompanied by a substantial reduction in sucrose levels due to a marked increase in net sucrose cleavage activity. Complementarily, *VaAPL1*-overexpressed (a key enzyme in starch biosynthesis) tomato plants subjected to 6 °C for 24 h raised sucrose accumulation through increased expression of starch hydrolysis and sucrose synthesis genes, and showed improved cold tolerance (Liang et al., 2022). In line with these findings, our results showed that although sucrose levels in basil leaves increased during storage compared to the at-harvest day, the sucrose concentration was notably lower at 4 °C than at 12 °C in the first 6 days, before the quality dropped below consumer acceptance limit (Fig. 4). The low sucrose levels observed may indicate a depletion of carbohydrate storage pools or signal energy deficiency, though the exact mechanism remains unclear. These observations collectively suggest that, in chilled basil leaves, high sucrose catabolism could lead to CI, especially in the early stage of CI development.

Metabolic pathways that use carbohydrates from native sources and from non-carbohydrate precursors as energy substrates appear to be limited in chilled basil leaves. This is evidenced by the downregulation of the glycolysis, the gluconeogenesis pathway, which synthesises glucose from non-carbohydrate sources (Walker et al., 2021), and the glyoxylate and dicarboxylate metabolism pathways, which produce intermediates for gluconeogenesis (Eastmond & Graham, 2001). Downregulation of these metabolic pathways in chilled basil leaves poses challenges in utilizing carbohydrates for energy production, leading to energy deficiency.

Likely to alleviate energy shortage, the citrate cycle (TCA cycle), propanoate metabolism, butanoate metabolism, and fatty acid biosynthesis pathways were upregulated in basil leaves stored at 4 °C (Fig. 5). Apparently, basil leaves rely more on alternative energy production pathways under chilling conditions, namely utilizing non-carbohydrate sources, for example fatty acids, to feed into the TCA cycle to compensate for the downregulation of glycolysis. This could be an adaptive response of basil to maintain cellular energy status through alternative non-carbohydrate substrates when carbohydrate substrates are limited by chilling stress. In addition, the energy status of cells is postulated to be critically linked to CI, as chilling stress has been reported to result in a decrease in ATP, ADP, and energy charge levels, as well as a reduction in the enzymatic activities associated with energy status (Chen et al., 2024; Vichaiya et al., 2022). Decreased efficiency in cellular energy generation and inadequate energy supply have also been shown to cause an increase in ROS production, promote membrane lipid hydrolysis and hinder membrane lipid biosynthesis, leading to impaired membrane integrity and increased ion leakage (Lin et al., 2022; Lin et al., 2023; Pan et al., 2019). This is consistent with our results showing the upregulation of fatty acid biosynthesis pathway and the downregulation of sphingolipid metabolism, glycerophospholipid metabolism, and glycerolipid metabolism pathways in chilled basil leaves (Fig. 5). The downregulation of these pathways also indicates a challenge to adjust membrane properties to cope with chilling stress (Zeng & Yao, 2022). Hence, although energy production via alternative non-carbohydrate sources, especially fatty acids released from the breakdown of membrane lipids, seems to be

activated, the intracellular energy level in chilled basil leaves is still inferred to be low. Moreover, energy deficiency could trigger autophagy and cell death (Iakimova et al., 2024). Therefore, the integration of energy- and membrane-related pathways in groups I and II (Fig. 5C) suggests a shortage in energy supply that may partly account for the membrane dysfunction and browning or blackening of tissues caused by CI in postharvest basil leaves.

During chilling stress, not only the cell membrane but also the cell wall framework may undergo extensive remodelling resulting in weakening. This was described in peach and nectarine fruits (Lurie, 2022). In our experiment, this was evidenced in chilled basil leaves by the downregulation of amino sugar and nucleotide sugar metabolism and galactose metabolism pathways, which play a central role in producing precursors for the main structural polysaccharides of cell wall (Figueroa et al., 2021). The reduced metabolic pathways in group II (Fig. 5C) suggests an impairment of cell membrane and cell wall integrity, leading to structural weakness under chilling stress.

4.3. *Carbohydrate flux prioritized for antioxidant defence system resulting in carbohydrate energy depletion*

Carbohydrate metabolism is essential for both energy production and antioxidant defence. The upregulation of starch and sucrose metabolism pathways (Fig. 5) in chilled basil leaves indicates a higher carbohydrate demand in response to chilling temperature. However, at the same time glycolysis is downregulated in chilled leaves and carbohydrates may therefore be redirected to other pathways, most likely the upregulated pentose phosphate pathway, as the latter runs parallel to glycolysis and competes with it to generate reducing equivalents in the form of NADPH and ribose 5-phosphate (Guo et al., 2019). This redistribution of carbohydrate substrates as a response to cold stress has also been reported in hydrogen sulphide treated peach fruit. Hydrogen sulphide treatment alleviated CI in peaches by inhibiting enzyme activities and substrate consumption in glycolysis, increasing the proportion of carbohydrate flux to the pentose phosphate pathway to generate sufficient NADPH, and enhancing the activity of ATPases, ensuring higher levels of ATP and energy charge (Wang et al., 2023). As the disruption of metabolic balance between energy production and antioxidant defence processes can lead to physiological disorders (Lurie, 2022), we hypothesize that basil leaves attempt to allocate more carbohydrate substrates to fuel protective mechanisms under cold storage, but this redistribution inadvertently leads to energy depletion, ultimately causing CI symptoms.

The group III (Fig. 5) antioxidant defence and stress response pathways exhibited enrichment patterns consistent with those observed in tomato and pepper plants under cold stress (Liang et al., 2022; Zhang et al., 2022). The upregulation of pentose phosphate pathway, lipoic acid metabolism, glutathione metabolism, and selenocompound metabolism pathways indicates an increased effort to combat oxidative stress caused by chilling (Navari-Izzo et al., 2002; Wen et al., 2024). Additionally, ribose 5-phosphate is a product of the pentose phosphate pathway that supplies ribose for nucleotide synthesis (Kruger & Von Schaewen, 2003). Purine metabolism pathway from group IV also plays a role in the synthesis of nucleotides (Witte & Herde, 2019). The simultaneous upregulation of pentose phosphate pathway and purine metabolism pathway implies nucleotide damage caused by chilling stress, necessitating enhanced synthesis for repair processes. The ubiquinone and other terpenoid-quinone biosynthesis pathway is also part of the antioxidant defence system and is crucial for electron transport (Liu & Lu, 2016). The downregulation of this pathway suggests reduced energy production and a diminished capacity to maintain cellular redox balance. The upregulation of arginine and proline metabolism resulted in enhanced level of proline, an osmoprotectants, under chilling stress (Fig. 4 & Fig. 5). However, the downregulation of most stress-related amino acid metabolism pathways reflects a reduced capacity to synthesize proteins and secondary metabolites critical for stress protection, e.g. the reduction of VOCs could be due to downregulated phenylalanine, tyrosine and tryptophan biosynthesis pathway (Kumar et al., 2021). This could also signify the importance of the arginine and proline metabolism and the alanine, aspartate, and glutamate metabolism pathways to chilling tolerance, as basil may prioritize the utilization of these key pathways over others in response to chilling stress.

While the importance of antioxidant defence systems to chilling tolerance is well recognized, the role of sugar metabolism in CI development, especially in the early stages, may be undervalued. Apart from their primary roles as an energy source and substrate for cellular processes, previous studies mostly identified carbohydrates as osmoprotectants, antioxidants, and by their role in supporting membrane function by interacting with lipid bilayer in response to cold stress (Bolouri-Moghaddam et al., 2010; Morelli et al., 2003; Sami et al., 2016), Given that most of the enriched antioxidant pathways were upregulated in this study, alongside the decreased level of H_2O_2 shown in our previous studies (Larsen et al., 2022a; Larsen et al., 2022b), it is possible that basil's antioxidant system might be sufficiently activated to maintain redox balance in the early exposure to chilling stress, despite overproduction of ROS. However, this activation could rely heavily on the supply of carbohydrate substrates, which simultaneously leads to a deficiency in carbohydrates available for energy metabolism. Therefore, we hypothesize that insufficient antioxidant capacity was not the cause of CI initiation in postharvest basil leaves; rather, the substrate imbalance between antioxidant and energy metabolisms, where the diversion of carbohydrate substrate flux towards the antioxidant defence system resulted in energy depletion and contributed to the initiation of CI in basil. This hypothesis is summarized in Fig. 6. Still, it remains an open question whether energy depletion is a single trigger that initiate other events, or if multiple events happen simultaneously.

To thoroughly test our primary hypothesis, future research should include measurements of ATP, ADP, and energy charge to assess the energy status during CI development. Additionally, the activities of enzymes involved in glycolysis and pentose phosphate pathway should be quantified. Given the observed depletion of ascorbic acid and rosmarinic acid and several enhanced antioxidant defence pathways, future studies should also address enzymatic antioxidant activities. Generally, low-temperature storage is known to suppress enzymatic activity and respiration; however, chilling stress has been associated with increased activity of sucrose cleavage, leading to a reduction in sucrose levels. The TCA cycle is central to cellular respiration and energy production. Enhanced TCA cycle activity in our study suggests that basil leaves may increase respiration to maintain energy balance under chilling stress. Elevated respiration at chilling temperature has also been reported in a sweet basil cultivar (Fratianni et al., 2017). Therefore, measuring both respiration and the enzymatic activities related to sucrose metabolism could provide more insights. Moreover, to better explore the incipience of CI, more focus should be placed on examining metabolic changes on a daily or hourly basis, as rapid and early chilling responses are often overlooked. Finally, quantifying and comparing shifts in energy and carbohydrate metabolism in basil with non-chilling-sensitive herbs, such as parsley and sage, under chilling storage conditions could further enhance our understanding of the mechanisms triggering CI.

5. Conclusion

Our findings suggest that CI in basil is associated with the redirection of carbohydrate substrates towards the antioxidant defence system, leading to energy depletion. Drawing from these results, we hypothesize that energy depletion acts as a primary trigger for CI in postharvest basil leaves. This indicates that managing carbohydrate flux could be critical for enhancing basil's chilling tolerance, potentially informing more effective cold storage strategies. While the role of carbohydrates in alleviating CI is recognized, their function as energy sources and substrates for antioxidant defence processes during CI development is often overlooked. Furthermore, it remains unclear whether energy depletion

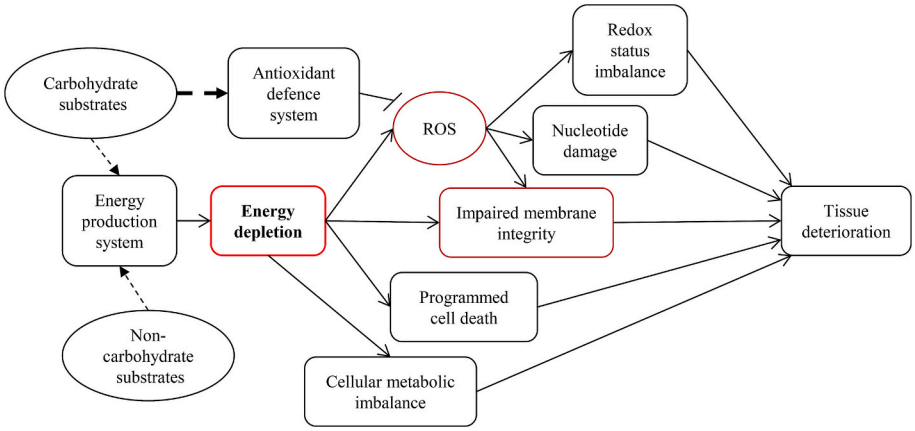


Fig. 6. Concept map illustrating the key relationships and processes underlying the hypothesized mechanism of chilling injury (CI) development in basil leaves. It is hypothesized that, during the CI initiation stage, an increase in carbohydrate substrate flux to the antioxidant defence systems and a decrease in flux to the energy production systems lead to energy depletion and therefore trigger CI. With energy depletion and insufficient antioxidant activity to scavenge reactive oxygen species (ROS), CI becomes severe. Cellular metabolic imbalance, redox status imbalance, nucleotide damage, impaired membrane integrity, and programmed cell death take place and lead to tissue deterioration. Dashed arrows represent substrate flux, with thicker arrows indicating greater flux. Solid lines depict relationships, where arrowheads indicate positive effects and blunt end indicates negative effects. Ovals represent metabolites, while rounded rectangles represent processes.

alone triggers CI or acts in conjunction with other factors. Overall, this research sheds light on the initiation mechanisms of CI, offering a new perspective for future studies.

Funding sources

This research is part of the TTW Perspectief programme "Sky High", which is supported by AMS Institute, Bayer, Bosman van Zaal, Certhon, Fresh Forward, Grodan, Growy, Own Greens/Vitroplus, Priva, Philips by Signify, Solynta, Unilever, van Bergen Kolpa Architects, and the Dutch Research Council (NWO).

Declaration of generative AI and AI-assisted technologies in the writing process

During the preparation of this work the authors used ChatGPT in order to improve language. After using this tool, the authors reviewed and edited the content as needed and take full responsibility for the content of the publication.

CRediT authorship contribution statement

Dorthe H. Larsen: Writing – original draft, Methodology, Conceptualization. **Ying Liu:** Writing – review & editing, Writing – original draft, Visualization, Investigation, Formal analysis. **Miaomiao Yao:** Writing – review & editing, Investigation. **Özlem Erol:** Writing – original draft, Visualization, Formal analysis, Data curation. **Yongran Ji:** Writing – review & editing, Investigation. **Ernst J. Woltering:** Writing – review & editing, Supervision, Conceptualization. **Leo F.M. Marcelis:** Writing – review & editing, Funding acquisition. **Young Hae Choi:** Writing – review & editing, Writing – original draft, Visualization, Supervision, Formal analysis, Data curation.

Declaration of competing interest

The authors declare that they have no known competing financial interests or personal relationships that could have appeared to influence the work reported in this paper.

Acknowledgements

The authors would like to thank Ep Heuvelink for the statistical support; Paul Kusuma for feedback; Gerrit Stunnenberg, Taede Stoker and David Brink for their technical support in climate chambers.

Appendix A. Supplementary data

Supplementary data to this article can be found online at https://doi.org/10.1016/j.foodchem.2025.143581.

Data availability

Data underlying the article Basil Chilling Injury: Oxidative Stress or Energy Depletion (Original data) (4TU.ResearchData)

References

Afrina, A., Kato, M., Takagi, T., & Yamawaki, K. (2012). Alleviating chilling injury of sweet basil leaves after harvest. *Food Preservation Science, 38*(4), 225–228. https://doi.org/10.5891/jafps.38.225

Aksenov, A. A., Laponogov, I., Zhang, Z., Doran, S. L. F., Belluomo, I., Veselkov, D., … Veselkov, K. (2021). Auto-deconvolution and molecular networking of gas chromatography–mass spectrometry data. *Nature Biotechnology, 39*(2), 169–173. https://doi.org/10.1038/s41587-020-0700-3

Albornoz, K., Zhou, J., Yu, J., & Beckles, D. M. (2022). Dissecting postharvest chilling injury through biotechnology. *Current Opinion in Biotechnology, 78*, Article 102790. https://doi.org/10.1016/j.copbio.2022.102790

Blokhina, O., Virolainen, E., & Fagerstedt, K. V. (2003). Antioxidants, oxidative damage and oxygen deprivation stress: A review. *Annals of Botany, 91 Spec No(2)*, 179–194. https://doi.org/10.1093/aob/mcf118

Bolouri-Moghaddam, M. R., Le Roy, K., Xiang, L., Rolland, F., & Van den Ende, W. (2010). Sugar signalling and antioxidant network connections in plant cells. *The FEBS Journal, 277*(9), 2022–2037. https://doi.org/10.1111/j.1742-4658.2010.07633.x

Brindisi, L. J., & Simon, J. E. (2023). Preharvest and postharvest techniques that optimize the shelf life of fresh basil (*Ocimum basilicum* L.): A review. *Frontiers in Plant Science, 14*, 1237577. https://doi.org/10.3389/fpls.2023.1237577

Cao, S., Yang, Z., Cai, Y., & Zheng, Y. (2011). Fatty acid composition and antioxidant system in relation to susceptibility of loquat fruit to chilling injury. *Food Chemistry, 127*(4), 1777–1783. https://doi.org/10.1016/j.foodchem.2011.02.059

Chambers, M. C., Maclean, B., Burke, R., Amodei, D., Ruderman, D. L., Neumann, S., … Mallick, P. (2012). A cross-platform toolkit for mass spectrometry and proteomics. *Nature Biotechnology, 30*(10), 918–920. https://doi.org/10.1038/nbt.2377

Chen, G., Kuang, X., Fan, Z., Chen, Y., Lin, Y., Wang, H., Chen, Y., & Lin, H. (2024). Energy and proline metabolisms participate in the occurrence of chilling injury in cold-stored Chinese olive fruit. *Postharvest Biology and Technology, 214*. https://doi.org/10.1016/j.postharvbio.2024.112955

Cozzolino, R., Pace, B., Cefola, M., Martignetti, A., Stocchero, M., Fratianni, F., Nazzaro, F., & De Giulio, B. (2016). Assessment of volatile profile as potential marker of chilling injury of basil leaves during postharvest storage. *Food Chemistry, 213*, 361–368. https://doi.org/10.1016/j.foodchem.2016.06.109

De Rocchis, V., Roitsch, T., & Franken, P. (2022). Extracellular glycolytic activities in root endophytic Serendipitaceae and their regulation by plant sugars. *Microorganisms, 10*(2), 320. https://doi.org/10.3390/microorganisms10020320

Dudai, N., Naharan, O., Bernstein, N., Shachter, A., Rud, R., & Chaimovitsh, D. (2017). Reduction of visible chilling injury in sweet basil (*Ocimum basilicum* L.) using artificial illumination. *Journal of Applied Research on Medicinal and Aromatic Plants, 6*, 15–21. https://doi.org/10.1016/j.jarmap.2016.12.002

Eastmond, P. J., & Graham, I. A. (2001). Re-examining the role of the glyoxylate cycle in oilseeds. *Trends in Plant Science, 6*(2), 72–78. https://doi.org/10.1016/S1360-1385(00)01835-5

Figueroa, C. M., Lunn, J. E., & Iglesias, A. A. (2021). Nucleotide-sugar metabolism in plants: The legacy of Luis F. Leloir. *Journal of Experimental Botany, 72*(11), 4053–4067. https://doi.org/10.1093/jxb/erab109

Fratianni, F., Cefola, M., Pace, B., Cozzolino, R., De Giulio, B., Cozzolino, A., … Nazzaro, F. (2017). Changes in visual quality, physiological and biochemical parameters assessed during the postharvest storage at chilling or non-chilling temperatures of three sweet basil (*Ocimum basilicum* L.) cultivars. *Food Chemistry, 229*, 752–760. https://doi.org/10.1016/j.foodchem.2017.02.137

Guo, X., Luo, T., Han, D., & Wu, Z. (2019). Analysis of metabolomics associated with quality differences between room-temperature- and low-temperature-stored litchi pulps. *Food Science & Nutrition, 7*(11), 3560–3569. https://doi.org/10.1002/fsn3.1208

Hou, Y., Li, Z., Zheng, Y., & Jin, P. (2021). Effects of $CaCl_2$ treatment alleviates chilling injury of loquat fruit (*Eribotrya japonica*) by modulating ROS homeostasis. *Foods, 10*(7). https://doi.org/10.3390/foods10071662

Hu, M., Shi, Z., Zhang, Z., Zhang, Y., & Li, H. (2012). Effects of exogenous glucose on seed germination and antioxidant capacity in wheat seedlings under salt stress. *Plant Growth Regulation, 68*(2), 177–188. https://doi.org/10.1007/s10725-012-9705-3

Iakimova, E. T., Ty, A. J., Hertog, M. L. A. T. M., Nicolaï, B. M., & Woltering, E. J. (2024). Programmed cell death and postharvest deterioration of fresh horticultural products. *Postharvest Biology and Technology, 214*. https://doi.org/10.1016/j.postharvbio.2024.113010

Kanehisa, M., & Goto, S. (2000). KEGG: Kyoto encyclopedia of genes and genomes. *Nucleic Acids Research, 28*(1), 27–30. https://doi.org/10.1093/nar/28.1.27

Kruger, N. J., & Von Schaewen, A. (2003). The oxidative pentose phosphate pathway: Structure and organisation. *Current Opinion in Plant Biology, 6*(3), 236–246. https://doi.org/10.1016/S1369-5266(03)00039-6

Kumar, V., Elazari, Y., Ovadia, R., Bar, E., Nissim-Levi, A., Carmi, N., Lewinsohn, E., & Oren-Shamir, M. (2021). Phenylalanine treatment generates scent in flowers by increased production of phenylpropanoid-benzenoid volatiles. *Postharvest Biology and Technology, 181*, Article 111657. https://doi.org/10.1016/j.postharvbio.2021.111657

Lange, D. D., & Cameron, A. C. (1994). Postharvest shelf life of sweet basil (*Ocimum basilicum*). *HortScience, 29*(2), 102–103. https://doi.org/10.21273/hortsci.29.2.102

Lange, D. L., & Cameron, A. C. (1997). Pre-and postharvest temperature conditioning of greenhouse-grown sweet basil. *HortScience, 32*(1), 114–116. https://doi.org/10.21273/HORTSCI.32.1.114

Larsen, D. H., Li, H., Shrestha, S., Verdonk, J. C., Nicole, C. C., Marcelis, L. F., & Woltering, E. J. (2022). Lack of blue light regulation of antioxidants and chilling tolerance in basil. *Frontiers in Plant Science, 13*, Article 852654. https://doi.org/10.3389/fpls.2022.852654

Larsen, D. H., Li, H., van de Peppel, A. C., Nicole, C. C. S., Marcelis, L. F. M., & Woltering, E. J. (2022). High light intensity at end-of-production improves the nutritional value of basil but does not affect postharvest chilling tolerance. *Food Chemistry, 369*, Article 130913. https://doi.org/10.1016/j.foodchem.2021.130913

Larsen, D. H., Marcelis, L. F. M., van Kempen, D., Kohlen, W., Nicole, C. C. S., & Woltering, E. J. (2023). Far-red light during cultivation improves postharvest chilling tolerance in basil. *Postharvest Biology and Technology, 198*, Article 112232. https://doi.org/10.1016/j.postharvbio.2022.112232

Li, H., Fan, Y., Zhi, H., Zhu, Y., Liu, Y., & Wang, Y. (2019). Influence of fruit stalk on reactive oxygen species metabolism and quality maintenance of peach fruit under chilling injury condition. *Postharvest Biology and Technology, 148*, 141–150. https://doi.org/10.1016/j.postharvbio.2018.10.018

Li, Z., Yong, B., Cheng, B., Wu, X., Zhang, Y., Zhang, X., & Peng, Y. (2019). Nitric oxide, gamma-aminobutyric acid, and mannose pretreatment influence metabolic profiles in white clover under water stress. *Journal of Integrative Plant Biology, 61*(12), 1255–1273. https://doi.org/10.1111/jipb.12770

Liang, G., Li, Y., Wang, P., Jiao, S., Wang, H., Mao, J., & Chen, B. (2022). *VaAPL1* promotes starch synthesis to constantly contribute to soluble sugar accumulation, improving low temperature tolerance in Arabidopsis and tomato. *Frontiers in Plant Science, 13*, Article 920424. https://doi.org/10.3389/fpls.2022.920424

Liang, S.-M., Kuang, J.-F., Ji, S.-J., Chen, Q.-F., Deng, W., Min, T., Shan, W., Chen, J.-Y., & Lu, W.-J. (2020). The membrane lipid metabolism in horticultural products suffering chilling injury. *Food Quality and Safety, 4*(1), 9–14. https://doi.org/10.1093/fqsafe/fyaa001

Lin, D., Yan, R., Xing, M., Liao, S., Chen, J., & Gan, Z. (2022). Fucoidan treatment alleviates chilling injury in cucumber by regulating ROS homeostasis and energy metabolism. *Frontiers in Plant Science, 13*, 1107687. https://doi.org/10.3389/fpls.2022.1107687

Lin, Y., Lin, L., Lin, Y., Lin, M., Ritenour, M. A., & Lin, H. (2023). Comparison between two cultivars of longan fruit cv. "Dongbi" and "Fuyan" in the metabolisms of lipid and energy and its relation to pulp breakdown. *Food Chemistry, 398*, Article 133885. https://doi.org/10.1016/j.foodchem.2022.133885

Liu, J., Li, Q., Chen, J., & Jiang, Y. (2020). Revealing further insights on chilling injury of postharvest bananas by untargeted lipidomics. *Foods, 9*(7), 894. https://doi.org/10.3390/foods9070894

Liu, M., & Lu, S. (2016). Plastoquinone and ubiquinone in plants: Biosynthesis, physiological function and metabolic engineering. *Frontiers in Plant Science, 7*, 1898. https://doi.org/10.3389/fpls.2016.01898

Lurie, S. (2022). Proteomic and metabolomic studies on chilling injury in peach and nectarine. *Frontiers in Plant Science, 13*, Article 958312. https://doi.org/10.3389/fpls.2022.958312

Majumder, A. L., Sengupta, S., & Goswami, L. (2010). Osmolyte regulation in abiotic stress. In *in abiotic stress adaptation in plants: physiological, molecular and genomic foundation* (pp. 349–370). https://doi.org/10.1007/978-90-481-3112-9_16

Meir, S., Ronen, R., Lurie, S., & Philosoph-Hadas, S. (1997). Assessment of chilling injury during storage: Chlorophyll fluorescence characteristics of chilling-susceptible and triazole-induced chilling tolerant basil leaves. *Postharvest Biology and Technology, 10*(3), 213–220. https://doi.org/10.1016/S0925-5214(97)01410-5

Meir, S., Twito, L., & Philosoph-Hadas, S. (1995). Correlation studies between chilling sensitivity of stored basil leaves and their composition of membrane lipids. In *In plant lipid metabolism* (pp. 381–383). https://doi.org/10.1007/978-94-015-8394-7_103

Morelli, R., Russo-Volpe, S., Bruno, N., & Lo Scalzo, R. (2003). Fenton-dependent damage to carbohydrates: Free radical scavenging activity of some simple sugars. *Journal of Agricultural and Food Chemistry, 51*(25), 7418–7425. https://doi.org/10.1021/jf030172q

Navari-Izzo, F., Quartacci, M. F., & Sgherri, C. (2002). Lipoic acid: A unique antioxidant in the detoxification of activated oxygen species. *Plant Physiology and Biochemistry, 40*(6–8), 463–470. https://doi.org/10.1016/S0981-9428(02)01407-9

Noguchi, A., Ito, S., Baba, T., & Ikeda, F. (2005). Changes in antioxidant activity and total phenol content during storage of sweet basil. *Food Preservation Science, 31*(6), 315–317. https://doi.org/10.5891/jafps.31.315

Pan, Y., Zhang, S., Yuan, M., Song, H., Wang, T., Zhang, W., & Zhang, Z. (2019). Effect of glycine betaine on chilling injury in relation to energy metabolism in papaya fruit during cold storage. *Food Science & Nutrition, 7*(3), 1123–1130. https://doi.org/10.1002/fsn3.957

Pang, Z., Lu, Y., Zhou, G., Hui, F., Xu, L., Viau, C., … Xia, J. (2024). MetaboAnalyst 6.0: Towards a unified platform for metabolomics data processing, analysis and interpretation. *Nucleic Acids Research, 52*(W1), W398–W406. https://doi.org/10.1093/nar/gkae253

Rodeo, A. J. D., & Mitcham, E. J. (2023). Chilling temperatures and controlled atmospheres alter key volatile compounds implicated in basil aroma and flavor. *Frontiers in Plant Science, 14*, 1218734. https://doi.org/10.3389/fpls.2023.1218734

Sami, F., Yusuf, M., Faizan, M., Faraz, A., & Hayat, S. (2016). Role of sugars under abiotic stress. *Plant Physiology and Biochemistry, 109*, 54–61. https://doi.org/10.1016/j.plaphy.2016.09.005

Stein, O., & Granot, D. (2018). Plant fructokinases: Evolutionary, developmental, and metabolic aspects in sink tissues. *Frontiers in Plant Science, 9*, 339. https://doi.org/10.3389/fpls.2018.00339

Sumner, L. W., Amberg, A., Barrett, D., Beale, M. H., Beger, R., Daykin, C. A., … Viant, M. R. (2007). Proposed minimum reporting standards for chemical analysis. *Metabolomics, 3*(3), 211–221. https://doi.org/10.1007/s11306-007-0082-2

Tang, D., Chen, M., Huang, X., Zhang, G., Zeng, L., Zhang, G., … Wang, Y. (2023). SRplot: A free online platform for data visualization and graphing. *PLoS One, 18*(11), Article e0294236. https://doi.org/10.1371/journal.pone.0294236

Vichaiya, T., Faiyue, B., Rotarayanont, S., Uthaibutra, J., & Saengnil, K. (2022). Exogenous trehalose alleviates chilling injury of 'Kim Ju' guava by modulating soluble sugar and energy metabolisms. *Scientia Horticulturae, 301*. https://doi.org/10.1016/j.scienta.2022.111138

Walker, R. P., Chen, Z.-H., & Famiani, F. (2021). Gluconeogenesis in plants: A key Interface between organic acid/amino acid/lipid and sugar metabolism. *Molecules, 26*(17), 5129. https://doi.org/10.3390/molecules26175129

Wang, K., Shao, X., Gong, Y., Zhu, Y., Wang, H., Zhang, X., Yu, D., Yu, F., Qiu, Z., & Lu, H. (2013). The metabolism of soluble carbohydrates related to chilling injury in peach fruit exposed to cold stress. *Postharvest Biology and Technology, 86*, 53–61. https://doi.org/10.1016/j.postharvbio.2013.06.020

Wang, L., Huang, X., Liu, C., Zhang, C., Shi, K., Wang, M., Wang, Y., Song, Q., Chen, X., Jin, P., & Zheng, Y. (2023). Hydrogen sulfide alleviates chilling injury by modulating respiration and energy metabolisms in cold-stored peach fruit. *Postharvest Biology and Technology, 199*. https://doi.org/10.1016/j.postharvbio.2023.112291

Wang, M., Carver, J. J., Phelan, V. V., Sanchez, L. M., Garg, N., Peng, Y., … Bandeira, N. (2016). Sharing and community curation of mass spectrometry data with global natural products social molecular networking. *Nature Biotechnology, 34*(8), 828–837. https://doi.org/10.1038/nbt.3597

Wen, Y., Cheng, L., Zhao, Z., An, M., Zhou, S., Zhao, J., … Yin, M. (2024). Transcriptome and co-expression network revealed molecular mechanism underlying selenium response of foxtail millet (Setaria italica). *Frontiers in Plant Science, 15*, 1355518. https://doi.org/10.3389/fpls.2024.1355518

Witte, C.-P., & Herde, M. (2019). Nucleotide metabolism in plants. *Plant Physiology, 182*(1), 63–78. https://doi.org/10.1104/pp.19.00955

Wongsheree, T., Ketsa, S., & van Doorn, W. G. (2009). The relationship between chilling injury and membrane damage in lemon basil (*Ocimum*×*citriodourum*) leaves. *Postharvest Biology and Technology, 51*(1), 91–96. https://doi.org/10.1016/j.postharvbio.2008.05.015

Wright, M., & Simon, E. W. (1973). Chilling injury in cucumber leaves. *Journal of Experimental Botany, 24*(2), 400–411. https://doi.org/10.1093/jxb/24.2.400

Yu, F., Ni, Z., Shao, X., Yu, L., Liu, H., Xu, F., & Wang, H. (2015). Differences in sucrose metabolism in peach fruit stored at chilling stress versus nonchilling stress temperatures. *HortScience, 50*(10), 1542–1548. https://doi.org/10.21273/HORTSCI.50.10.1542

Zeng, H.-Y., & Yao, N. (2022). Sphingolipids in plant immunity. *Phytopathology Research, 4*(1), 20. https://doi.org/10.1186/s42483-022-00125-1

Zhang, J., Liang, L., Xie, Y., Zhao, Z., Su, L., Tang, Y., … Li, H. (2022). Transcriptome and metabolome analyses reveal molecular responses of two pepper (*Capsicum annuum* L.) cultivars to cold stress. *Frontiers in Plant Science, 13*, Article 819630. https://doi.org/10.3389/fpls.2022.819630

Zhang, W., Jiang, H., Cao, J., & Jiang, W. (2021). Advances in biochemical mechanisms and control technologies to treat chilling injury in postharvest fruits and vegetables. *Trends in Food Science & Technology, 113*, 355–365. https://doi.org/10.1016/j.tifs.2021.05.009

Zhao, Y., Tang, J., Brummell, D. A., Song, C., Qi, S., Lin, Q., … Duan, Y. (2022). Abscisic acid alleviates chilling injury in cold-stored peach fruit by regulating the metabolism of sucrose. *Scientia Horticulturae, 298*. https://doi.org/10.1016/j.scienta.2022.111000